International Journal of Mechanical and Production Engineering Research and Development (IJMPERD)
ISSN(P): 2249-6890; ISSN(E): 2249-8001
Vol. 9, Issue 4, Aug 2019, 777-784
© TJPRC Pvt. Ltd.

THE FLOW VISUALIZATION OF SMALL-SCALE AIRCRAFT ENGINE AXIAL FLOW TURBINE ROTOR USING NUMERICAL TECHNIQUE

VARUN CHIVUKULA[1], RUCHIKA MOHLA[2] & SRINIVAS. G[3*]

[1,2]*Student, Department of Aeronautical and Automobile Engineering, Manipal Institute of Technology, Manipal, Karnataka, India*

[3]*Assistant Professor, Department of Aeronautical and Automobile Engineering, Manipal Institute of Technology, Manipal, Karnataka, India*

ABSTRACT

The axial flow turbine is widely used in gas turbines for expansion of hot gases emerging from the combustion chamber. The turbine expands the flow and generates power to drive the compressor and fan. The designing needs to accommodate high speeds and altitudes, as well as reduce losses in order to improve stage efficiency and overall efficiency. Some of the problems are tip leakage flow, high thermal loads on the blades, airfoil erosion, etc. The present paper involves basic flow simulation of a small-scale aircraft engine axial flow turbine rotor (full annulus) using ANSYS CFX at standard atmospheric conditions in order to study as well as predict the unsteady characteristics and in the future, to find a solution to curb the unsteadiness found. This paper will be useful for anyone who wants to get a basic idea of modelling and performing analysis for any turbo machinery component using a numerical technique.

KEYWORDS: Axial Flow Turbine, Gas Turbine, Numerical, Approach, CFD & CFX

Received: May 18, 2018; **Accepted:** Jun 08, 2019; **Published:** Jul 10, 2019; **Paper Id.:** IJMPERDAUG201978

Original Article

INTRODUCTION

An axial turbine is a continuous arrangement of rotor-stator, where mechanical energy is obtained by converting the kinetic energy produced from the fluid flow. Based on the power requirement, an axial flow turbine can either be single-staged or multi-staged. Axial flow turbines are more efficient and can handle large mass flow rates. Available pressure ratios and allowable blade stress in turning determine the turbine work per stage ratio.

Turbine blades have high camber and are set at negative stagger. Turbine blades require high blade loadings and cooling. Even number of blades are used in rotors for ease of balancing and odd (preferably prime number) of blades are used in stator. A large number of rotor blades are used to minimize the length of the engine where as, number of stator blades is relatively smaller. Also the blades are hollow to minimize the weight penalty.

In case of less number of blades a large camber or turning is used, and high stagnation pressure losses are attained for flow separation on suction surface. Whereas, for more number of blades smaller camber or turning is used and high stagnation pressure is attained for larger surface area with frictional losses. As the demand for turbines has been increasing, a study of turbine aerodynamic load enhancing for low aspect ratio turbine blades was a necessity. Upto 30-50% of total loss of efficiency for turbine blade row with low aspect ratio, are end-wall losses (usually termed secondary flow losses or secondary losses). In the designing of turbine blades, the major problem that arises is the grasping capability, analysis, estimation and resistance of secondary flows.

The new turbines have lesser blades with greater loading. The blades are slender, bigger, are with little gaps and have greater stage loading. Water injection at the inlet or between sections, which will likely affect airfoil erosion life, is one of the new ideas. The event of encountering rubs is highly likely because of minute clearances and greater pressure ratios. The new turbine blades have squealer segments on the tip of the blades, which wear out if the blades come in touch with the casing. These squealers sometimes lead to fracture of the tips and damage of entire diffuser vanes and downstream blades due to severe domestic object damage. Design tallies, set by Finite Element Modelling (FEM), at the component level leads to lower safety margins as compared to early designs. The costs of these airfoils is mostly high and there are no factors that reduce the happening of these failures and reduce the effects, when modern gas turbines are observed from a hazard standpoint. In order to aid the fast growing research in the field of propulsion, significant work needs to be available in open literature about the basic steps necessary to carry out analysis, which is covered in this paper.

LITERATURE REVIEW

Review

Qi Lei et al. [1] studied the interaction mechanisms between streamwise and secondary vortex and also the vortex position impact on the performance of turbine cascade. Reduction of secondary flow losses using a streamwise vortex was the main aim. A numerical as well as an experimental analysis was done on the turbine cascade. The results showed a decline in the stagnation pressure loss as well as the flow deviation, and also it showed a significant relation between this decline and the location of streamwise vortex.

Qi Lei et al. [2] investigated the end-wall region of turbine and the unsteady interaction of secondary flow vortices by introducing an upstream periodic wake. This study was done both experimentally and numerically on a linear turbine cascade and a turbine rotor. The results showed the physical mechanisms of unsteady interaction between secondary vortices and upstream wake and its effect on performance of turbine end wall region.

Daniel J. Dorney et al. [3] performed various experiments and simulations on low pressure turbine blades at different Reynolds number to carefully observe the behavior of turbine and fluid flow around the turbine. The results showed an increase in cascade losses with a decrease in Reynolds number. Also it was observed that altering the boundary layer helped reducing the losses at low Reynolds numbers.

J. Cui et al. [4] studied the effect of three different inflow conditions from an upstream blade row which are turbulent boundary layer (TBL), wakes with secondary flow (W&S) and laminar boundary layer (LBL). Use of precursor eddy resolving simulations was used to imitate realistic inflows. It was observed that incoming wakes along with the secondary flow led to an incline in local loss generation rate at end-wall as well as mid-span of the blade passage in the frontal area. Also at the aft of passage the wakes suppressed the formation of separation bubble at mid-span hence decreasing the local loss generation rate. The wakes shed from trailing edge mix more rapidly in mid-span than in end-wall.

JieGao et al. [5] studied the unsteady end-wall flow interactions in shrouded and unshrouded turbines with the use of three-dimensional Navier-Stokes viscous solver. Results showed that unsteady interactions led to a decrease in radial vorticity of turbine end-wall secondary flows, and that its effects on streamwise vorticity significantly depends on upstream wake characteristics. A proper control of unsteady interactions reduces the intensity and size of end-wall secondary flows, thus improving the turbine performance.

C. De Maesschalck et al.[6] performed numerical investigations i.e. RANS calculations on high pressure turbine stage at non dimensional parameters such as Mach number, Reynolds number and etc., using Numeca FINE/Turbo suite with SST turbulence model to investigate aerodynamic and heat transfer characteristics at the tip. A new change was observed in the aero-thermal characteristics in the over tip region which provided new physical insights, necessary for future design of efficient rotating machines with minimal leakage.

Jan Halama et al. [7] studied turbine cascades and stages by performing numerical simulations of steady and unsteady transonic flows. A finite volume, cell-vertex, time marching method was used to study the effects of numerical dissipation, grid quality and boundary condition approximation on numerical solution. Results showed that O–H multi-block grid eliminated the grid influence completely, but grid generation was very difficult. While the elliptic H-type grid suffered from wake-like structure, but also provided a decent distribution of quantities along the blade profile with a simpler generation procedure.

Vijay K. Garg et al. [8] did a computational study using the Glenn-HT code to analyze the use of vortex generator jets (VGJs) used in controlling the separation on low pressure turbine blade at low Reynolds number. Results showed that the code determined the correct location of separation point on the suction surface of blade (without any VGJ) at Reynolds numbers less than or equal to 50,000. Also, the code helped in concluding that the separated region vanishes if VGJs are used.

Summary of Literature Review

A comparison between experimental and numerical analysis has been done between various models of turbines to study the unsteady transonic flow around the turbine blades in both cascades and rotor-stator stages. Effects of different conditions have been tracked such as wake formation and vortex formations at different locations of turbine blades. For example in [1] effects of a delta wing generating vortices at frontal, mid-span and aft regions of turbine were tracked using a Shear Stress transport model on ANSYS software. In [4] a study on effects of three different inflow conditions from an upstream blade row was done. In [8] effects of vortex generator jets were tracked around a low pressure turbine blade to study the performance enhancement of turbines. Dependency of some such parameters with the performance of turbine was recorded to help in modelling of turbines in the future.

METHODOLOGY

Modeling

The geometry of the blade considered [1] has a large turning angle at the leading edge resulting in very strong passage vortex. This passage vortex was clearly captured in the analysis described subsequently. Also, full annulus case was considered for better understanding and for further detailing about the effects of flow on other blades. Table 1 showcases the details of the geometry of the airfoil presented in [1].

Table 1: Geometry Details of Turbine [1]

Sr. No.	Geometry	Measurement
1.	Number of blades	36
2.	Blade chord (mm)	112.9
3.	Blade axial chord (mm)	94.719
4.	Blade height (mm)	200
5.	Pitch (mm)	84.5
6.	Inlet angle (from axial)	50°

Table 2: Contd.,		
7.	Outlet angle (from axial)	-63.7°
8.	Inlet free stream turbulence	1%
9.	Exit velocity (m/s)	30
10.	Exit Reynolds number (axial chord)	2×10^5

The modelling of the blade was done using Blade Gen tool in ANSYS Workbench 18.1. The model, which had some anomalies due to limited information provided, was corrected using free hand sketch and image tracing tools. Figure 1is the airfoil used.

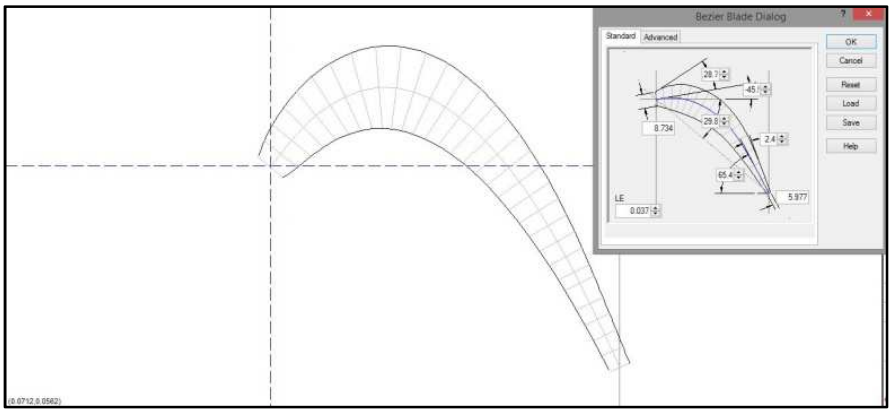

Figure 1: Representation of Airfoil on BladeGen

Meshing

ANSYS Turbo Grid was used to mesh the geometry. Global size factor was used to refine the mesh and a size factor of 2 was selected. At the inlet and outlet, a H-grid mesh type was used with 1.2 as the expansion rate. A good mesh was obtained near the blade, showcased in Figure 2 and 3, crucial for accuracy in the analysis. Figure 5 shows the mesh statistics. A total of nearly 1 million mesh elements resulted while meshing.

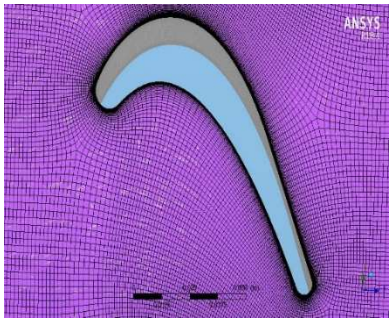

Figure 2: Close to Blade View of Meshing

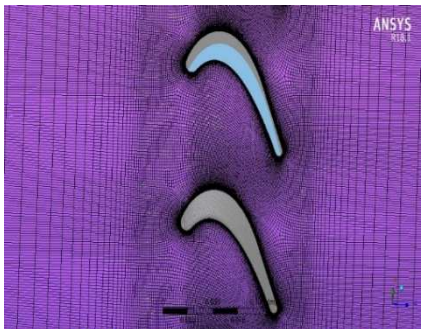

Figure 3: Blade-to-Blade View of The Mesh

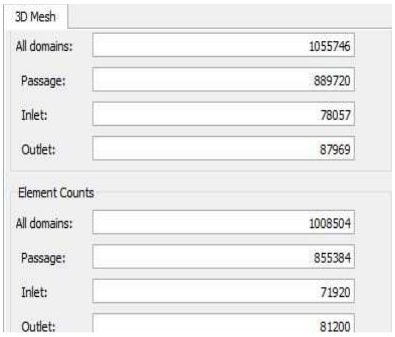

Figure 4: Mesh Statistics

Boundary Conditions and Numerical Technique

ANSYS CFX software was used to conduct a steady state analysis. Standard atmosphere conditions were considered i.e. air at 300K and 1 atm pressure. A total energy method and Shear Stress Transport (SST) turbulence model were selected. A mass flow inlet and P-static outlet boundary template were selected with mass flow rate at the inlet being 0.6 kg/s, calculated using the exit velocity given [1]. The rotor was calculated to be approximately operating at 591.726 rpm and turbulence intensity was kept at 1% and outlet was converted into an opening with 300K temperature to avoid

overflow (figure 5). Advection scheme and turbulence numeric were set to high resolution and RMS convergence criteria was selected with target being 10^{-4} (1e-4).

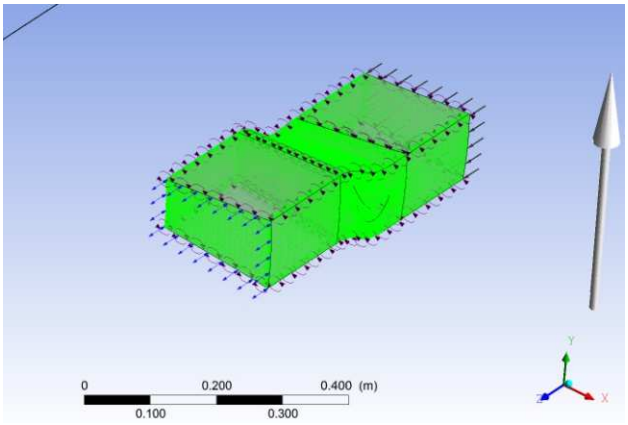

Figure 5: Flow Domain Subjected to Rotation

After close observation of the RMS residual values which attained a repetitive pattern, shown in figure 6, after over 550 iterations, the solver was stopped and decent enough results were achieved.

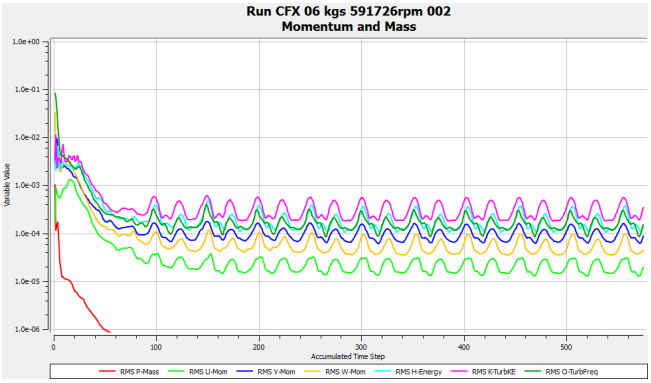

Figure 6: Momentum and Mass Residuals Convergence Plot

RESULTS AND DISCUSSIONS

Pressure

Figure 7, 8 & 9 show the contours of pressure clearly on the either side of the blade as well as on the hub and shroud. The pressure contours on the bottom and top surface of the blade showed the existence of high and low pressure respectively as well as a separation bubble at the bottom surface due to the high curvature/camber of the blade. The pressure near the hub and shroud showed distortion to a certain extent which is the consequence of flow separation and unsteady flow. The blade-to-blade view, shown in figure 10, represents the pressure interaction between the blades.

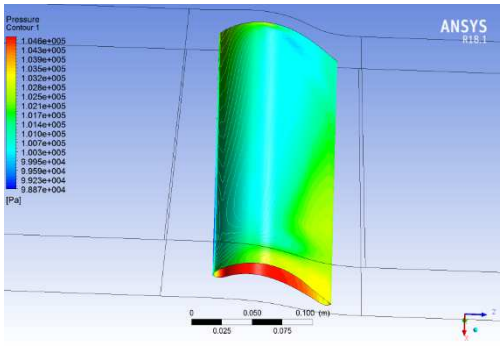

Figure 7: Pressure on Top Surface

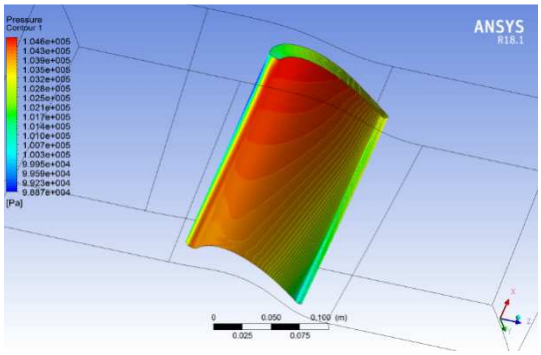

Figure 8: Pressure on Bottom Surface

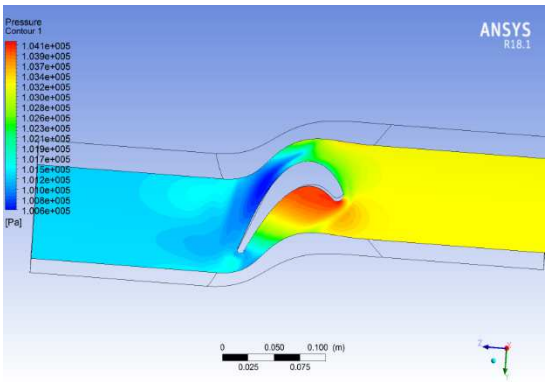

Figure 9: Pressure on Hub

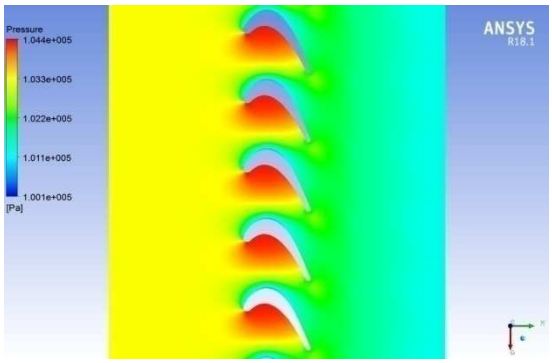

Figure 10: Blade-to-Blade View of Pressure on Shroud

Figure 11 shows the Cp plot vs chord length of the blade at mid-span. It indicates the presence of stagnation point at the leading edge and drop in suction side pressure at the trailing edge.

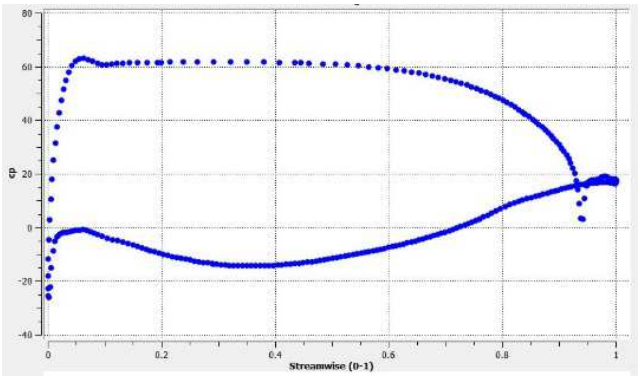

Figure 11: C_P plot

Velocity

Figures 12-15 show the streamlines and contours of velocity distribution. The velocity profile matches and is feasible with the pressure distribution as in, the bottom surface encounters low velocity and the top surface encounters high velocity. A very high velocity is observed right where the stagnation point was observed.

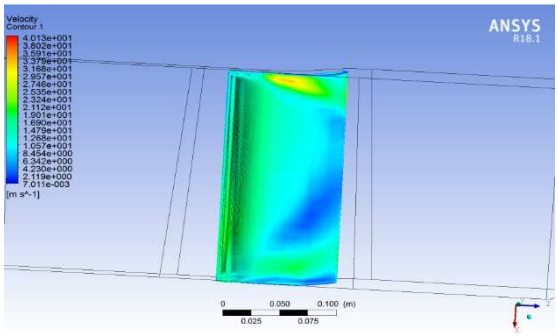

Figure 12: Velocity Contour on Top Surface

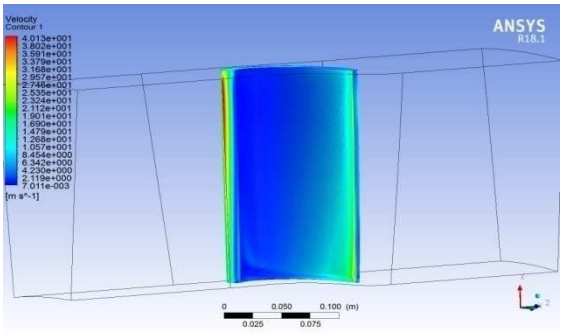

Figure 13: Velocity Contour on Bottom Surface

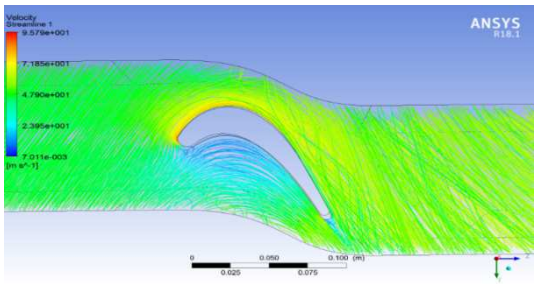

Figure 14: Velocity Streamline

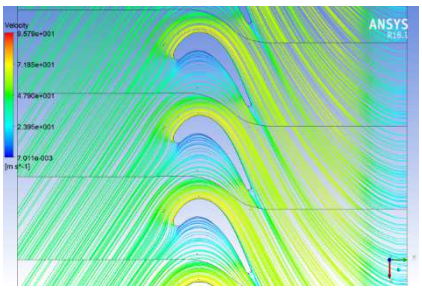

Figure 15: Blade-to-Blade View of Velocity Streamline

Vorticity

Figures 16,17 & 18 show the vorticity contours. Figure 16 is the 3D representation of the vortices which are predominantly formed at the hub and shroud due to leakage. Figures17 & 18 representing vorticity at the hub and shroud approve the same fact as the vorticity is maximum with a value of 1098.63 s^{-1} at the leading edge and trails backwards as the flow moves along.

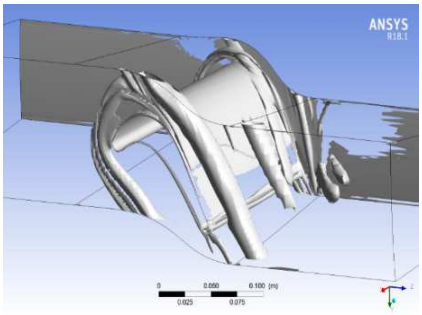

Figure 16: 3D View of Vorticity

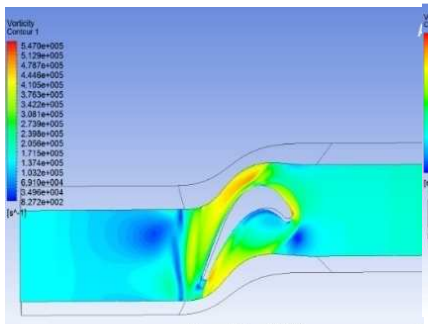

Figure 17: Vorticity at the Hub

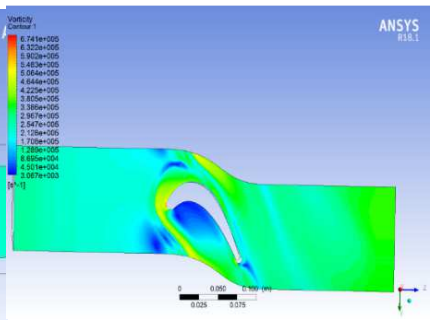

Figure 18: Vorticity at the Shroud

CONCLUSIONS

- The paper uses ANSYS CFX to capture the flow characteristics and behavior near the turbine blade at standard atmosphere conditions using steady state case.
- It was observed that due to the high blade loading and large turning angle, there were significantly strong vortices generated at the hub and shroud of the turbine.
- This paper gives a basic idea on how to approach the flow simulation of an axial flow turbine rotor using minimum boundary conditions and geometric details.

- The pressure, velocity and vorticity values and patterns attained are feasible and generally applicable validating the use of this research.
- Further research is recommended for improved visualization of the losses and solutions/techniques required for performance enhancement.

REFERENCES

1. *Qi Lei, Zou Zhengping, Wang Peng, Cao Teng, Liu Huoxing. Control of secondary flow loss in turbine cascade by stream-wise vortex. Computers & Fluids 54 (2012), 45-55.*
2. *Qi Lei, Zou Zhengping, Liu Huoxing, Li Wei. Upstream wake–secondary flow interactions in the end-wall region of high-loaded turbines. Computers & Fluids 39 (2010), 1575-1584.*
3. *Daniel J. Dorney, James P. Lake, Paul I. King, David E. Ashpis. Experimental and Numerical Investigation of Losses in Low-Pressure Turbine Blade Rows. NASA/TM-2000.*
4. *J. Cui, V. Nagabhushana Rao, P.G. Tucker. Numerical investigation of secondary flows in a high-lift low pressure turbine. International Journal of Heat and Fluid Flow 63 (2017), 149-157.*
5. *JieGao, Qun Zheng. Comparative investigation of unsteady flow interactions in end-wall regions of shrouded and unshrouded turbines. Computers & Fluids 105 (2014), 204-217.*
6. *Umesh, K. S., Pravin, V. K., & Rajagopal, K. (2014). Experimental Investigation and CFD Analysis of Multi-Cylinder Four Stroke SI Engine Exhaust Manifold for Optimal Geometry to Reduce Back Pressure and to Improve Fuel Efficiency. International Journal of Automobile Engineering Research and Development, 4, 13-20.*
7. *C. De Maesschalck, S. Lavagnoli, G. Paniagua, N. Vinha. Aerothermodynamics of tight rotor tip clearance flows in high-speed unshrouded turbines. Applied Thermal Engineering 65 (2014), 343-351.*
8. *Jan Halama, Tony Arts, Jaroslav Fort. Numerical solution of steady and unsteady transonic flow in turbine cascades and stages. Computers & Fluids 33 (2004) 729-740.*
9. *Vijay K. Garg. Low-Pressure Turbine Separation Control— Comparison with Experimental Data. NASA/CR-2002.*